

NOTAS DE FÍSICA

VOLUME II

Nº 10

EAST-WEST ASYMMETRY OF POSITIVE AND NEGATIVE MESONS  
AT THE GEOMAGNETIC EQUATOR

by

I. Escobar V,

and

F. B. Harris

CENTRO BRASILEIRO DE PESQUISAS FÍSICAS

Av. Wenceslau Braz, 71

RIO DE JANEIRO

1955

EAST-WEST ASYMMETRY OF POSITIVE AND NEGATIVE MESONS  
AT THE GEOMAGNETIC EQUATOR\* +

I. Escobar V.

Universidad Mayor de San Andrés

La Paz, Bolivia

and

Centro Brasileiro de Pesquisas Físicas

Rio de Janeiro, D. F.

and

F. B. Harris §

Massachusetts Institute of Technology

Laboratory for Nuclear Science

Cambridge, Massachusetts

(October 20, 1955)

The intensities of positive and negative  $\mu$  mesons at zenith angles of  $45^\circ$  in the east-west plane and at the vertical have

---

\* Supported in part by the joint program of the U.S. Office of Naval Research and the U.S. Atomic Energy Commission.

+ This paper will be published in the "Physical Review".

§ Now at Utica College of Syracuse University, Utica, New York.

been measured at atmospheric depth  $548 \text{ g cm}^{-2}$  near the geomagnetic equator. The data are analyzed through use of the empirical production spectrum and unidimensional equation for  $\mu$ -meson production employed by Sands and by Olbert. A careful theoretical discussion is given, taking into account in detail the various effects arising both from the variation of the geomagnetic cutoff with direction of incidence of the primaries and from the curvature of the trajectories of the mesons in the earth's magnetic field after their production in the atmosphere. It is found that, to bring  $45^\circ$  and vertical data into accord, it is necessary to assume an rms angle of production of the parent  $\pi$  mesons of  $14^\circ \pm 2^\circ$ . It is then possible to express the production spectrum, at any geographical location, by the single equation  $G(R') = A |R' + a(M_c)|^{-n}$ , where  $M_c$  is the cutoff magnetic rigidity for the primaries in a given direction of incidence at that location. The data do not indicate the presence of any appreciable number of negatively charged particles in the primary cosmic radiation.

## I. INTRODUCTION

The various directional asymmetries observed in the secondary cosmic radiation arise through two principal mechanisms. The first of these is the action of the magnetic field of the earth upon the primary particles. The second is the curvature in the same magnetic field, of the trajectories of the secondary particles after their production in the atmosphere.

Fortunately, it is possible mathematically to consider

the two processes as taking place consecutively, rather than concurrently. That is, the depth of the atmosphere is sufficiently small in comparison with the radii of curvature of those primary trajectories which are of interest that the primaries can be considered to undergo all of their deflection outside the atmosphere and to follow rectilinear trajectories after their entrance into the atmosphere. The secondaries however, much degraded in energy with respect to their primary parents, have considerable curvature in the magnetic field. The depth of the atmosphere is small enough compared with the radius of the earth that the portion of the earth's surface above which the secondary phenomena occur can be considered plane.

We shall follow Sands <sup>1</sup> and Olbert <sup>2-4</sup> in employing an empirical differential range spectrum of  $\mu$  mesons at production of the form

$$G(R') = A(a + R')^{-n}, \quad (1)$$

where  $R'$  is the range of the  $\mu$  meson at production. Sands derived values for the three constants of Eq. (1) on the basis of data on the vertical intensity at one latitude. Olbert reasoned that since very high-energy  $\mu$  mesons can come only from high-energy primaries, i.e., those which are not affected by the earth's magnetic field, the spectrum for large values of  $R'$  must be independent of position on the earth, provided the primary radiation in the neighborhood of the earth is isotropic. Now the only one of the three empirical constants in the foregoing expression to which  $G(R')$  is insensitive at large ranges is  $a$ , so that if indeed the empirical

expression for the production spectrum does have this same general form at all locations on the earth, the constants  $A$  and  $n$  must be the same everywhere. He thus extended Eq. (7) to apply to the vertical direction at various geomagnetic latitudes,  $a$  becoming a function of geomagnetic latitude. His values of the various parameters were based on more complete data than were Sands'.

The purpose of this paper is threefold: (a) to extend the range of applicability of Eq. (7) to include not only any location on the earth and any altitude, but also any direction of observation, (b) to relate  $a$  more precisely to the geomagnetic cutoff, and (c) to develop a theory whereby the intensities of positive and negative  $\mu$  mesons in a given direction may be separately computed and the primary and secondary effects on the east-west asymmetries understood.

## II. GEOMAGNETIC EFFECTS

The behavior of a particle in a magnetic field in vacuo depends exclusively upon its magnetic rigidity  $M$ , or ratio of momentum to charge. The magnetic rigidity in  $Bv$  is numerically equal to the momentum in  $Bev/c$  for singly charged particles, but of course not for multiply charged particles.

For a given direction of incidence at a particular location on the earth, the terrestrial magnetic field acts as a rigidity filter on the primary radiation. No particles having rigidity less than  $M_2$ , computed from either the Störmer cone or the simple shadow cone,<sup>5,6</sup> can reach the earth in the given direct-

ion. Particles of all rigidities greater than  $M_1$ , computed from the main cone, <sup>7,8</sup> can arrive from that direction. Between  $M_1$  and  $M_2$ , in the so-called "penumbra", some rigidities are allowed, others forbidden, the region ranging from mostly forbidden at the equator to mostly allowed at the poles. If, at a certain location, a given direction is accessible to particles of a certain rigidity, particles of that rigidity will arrive at the top of the atmosphere in that direction with the same intensity as that which they would have in the absence of the magnetic field. <sup>9,10</sup>

Since experimentally what is observed in the penumbra is some sort of "average" or effective intensity having a value between zero and the full intensity, in practice it is customary to define an effective "cutoff rigidity"  $M_c$  at a given location and in a given direction, above which all particles are assumed to arrive with full intensity and below which the intensity is zero.  $M_c$  is naturally intermediate in value between  $M_1$  and  $M_2$ , coinciding with  $M_1$  at very low latitudes and with  $M_2$  at very high latitudes. Curves of  $M_1$  and  $M_2$ , <sup>11</sup> and a tentative curve of  $M_c$ , at the vertical as functions of geomagnetic latitude are shown in Fig. 1, under the assumption of a centrally located magnetic dipole. In the east-west plane at the equator, the Störmer and main cones very nearly coincide, so that the simple Störmer theory holds approximately.

Actually the true field of the earth is much better represented by a dipole located at 342 km from the center. <sup>12</sup> For most purposes, the simplest procedure is to consider first the symmetrical case, and then make corrections for the eccentricity of

the dipole.

The magnitudes of the several critical rigidities mentioned above depend inversely upon the square of the radius of the earth. Hence, the most important correction which must be made upon the symmetrical case is that due to the fact that the actual distance from the observer on the surface of the earth to the eccentrically placed dipole is not equal to the radius of the earth. The fractional correction to one of the critical rigidities is given by the relation.

$$(\Delta M/M) = - 0.706 \cos \lambda \cos(\omega - 18.2^\circ), \quad (2)$$

where  $\lambda$  is the geomagnetic latitude and  $\omega$  the geomagnetic longitude.

A second but rather less important correction is due to the fact that the magnetic vertical, again because of the eccentric position of the dipole, does not coincide with the gravitational vertical. This correction can be applied properly only by referring all directions to a new meridian plane, which has been rotated through an angle  $\theta_m$  with respect to the geographical meridian plane, about an axis parallel to the axis of the earth's dipole. This angle can be computed as follows:

$$\sin \theta_m = 0.053 \sin(\omega - 18.2^\circ), \quad (3)$$

where a positive result indicates that the new reference plane lies east of the meridian plane. It is seen that the angle of rotation varies from zero to about  $3^\circ$ . At the vertical, one can derive the following approximate expression for the fractional correction due

to this effect, useful except at very high latitudes:

$$(\Delta M/M) = - 0.027 \sin(\omega - 18.2^\circ) \cos^3 \lambda \quad (4)$$

Thus we have, at the vertical, the following general expression:

$$M = M_0 \left[ 1 - 0.106 \cos(\omega - 18.2^\circ) \cos \lambda - 0.027 \sin(\omega - 18.2^\circ) \cos^3 \lambda \right], \quad (5)$$

where here  $M$  represents the corrected value of one of the critical<sup>1</sup> rigidities, either  $M_1$ ,  $M_2$ , or  $M_c$ , and  $M_0$  represents its uncorrected value (i.e., computed for the case of a centrally located dipole).

Geomagnetic latitude  $\lambda$  can be computed from the following expression:

$$\sin \lambda = \cos 78.5^\circ \cos(\Omega - 69.0^\circ) \cos \Lambda + \sin 78.5^\circ \sin \Lambda, \quad (6)$$

where  $\Lambda$  and  $\Omega$  are geographic latitude and longitude, respectively. The geomagnetic longitude  $\omega$  can be computed from a similar expression as follows:

$$\cos(\omega - 69.0^\circ) = (\cos \lambda)^{-1} \times \left[ \sin 78.5^\circ \cos(\Omega - 69.0^\circ) \cos \Lambda - \cos 78.5^\circ \sin \Lambda \right]. \quad (7)$$

In both the above formulas, west longitude and north latitude are considered positive.



### III. INTENSITY OF $\mu$ MESONS IN THE ATMOSPHERE

#### (a) Discussion

The intensity of  $\mu$  mesons observed in a given direction at a given atmospheric depth at a given location on the earth depends upon a large number of factors. The observed  $\mu$  mesons comprise contributions from  $\pi$  mesons decaying in flight at all atmospheric levels above the point of observation. Their energy at production is greater than that at observation by an amount determined by the ionization loss experienced in transit, and the fraction of those produced at a given level arriving at the level of observation is influenced by the survival probability of  $\mu$  mesons.

The  $\pi$  mesons decaying at any particular level have in turn been produced in nuclear interactions at all levels above that at which they decay. In addition to the considerations mentioned above for the case of  $\mu$  mesons, the number of  $\pi$  mesons succeeding in giving birth to  $\mu$  mesons depends also upon the cross section for nuclear interaction of  $\pi$  mesons.

The number of  $\pi$  mesons produced at a given level depends, of course, upon the intensity and composition of the nucleonic component at that level. If the primary particles are all of one sign, the character of the nucleonic component at the top of the atmosphere is determined, to a good order of approximation, only by the one parameter  $M_c$ , the effective cutoff rigidity. With Olbert,<sup>3</sup> we shall consider that this meson-producing component is then absorbed exponentially in the atmosphere with a mean free

path of  $127 \text{ g cm}^{-2}$ .

The intensity of  $\mu$  mesons in a given direction will thus depend not only upon the quantity of intervening material, but also upon the value of  $M_c$  in that direction. Since the survival probability depends chiefly upon linear spatial distance traversed, the intensity will depend also upon zenith angle due to the different density distribution found at an angle (if equal masses of intervening air are considered). For the same reason, it will depend upon the temperature distribution in the atmosphere above the point of observation. This last effect has been considered in some detail by Olbert. <sup>2,3</sup>

If one examines in more detail the problem of the paths of  $\mu$  mesons in the atmosphere, it becomes evident that the above analysis must be modified to take into account the fact that their trajectories are appreciably curved due to the action of the terrestrial magnetic field after their production. In other words, the  $\mu$  mesons observed in a certain direction have arisen from various points along a curved trajectory stretching back from the point of observation. Proceeding upward along this trajectory, the curvature is toward the east for positive mesons and toward the west for negatives. This problem was first studied by Rossi, <sup>13</sup> and later by Johnson <sup>14</sup> and Bowen. <sup>15</sup>

Olbert's computations, <sup>3,4</sup> for mesons having ranges between 700 and 6000  $\text{g cm}^{-2}$  at sea level, assume that the parent  $\pi$  mesons decay instantaneously and that the direction of the primary particle is preserved in the  $\pi$  - and  $\mu$  -meson production processes. Even with this simplification, the curvature of path pro-

foundly complicates the computation of the  $\mu$ -meson intensities, especially at directions other than the vertical.

Let us consider, for example, mesons arriving from some zenith angle in the east. The positives come in along a trajectory which bends farther away from the vertical as one moves upward, while the negatives follow a trajectory which bends closer to the vertical at the higher altitudes. Comparing positives and negatives born at the same altitude, one sees that the negatives on the average have traversed a shorter distance and a smaller mass of air than the positives, giving rise to two effects: (a) the negatives on the average have lower energies at birth than the positives, and (b) the survival probability of the negatives is greater on the average than of the positives. Both these effects tend to favor the negatives. It must be borne in mind that the mesons observed come from all points of the trajectory, and that therefore the total number will depend upon a summation of all such contributions. The positive trajectory is longer than the negative, i.e., a greater mass of air is available in which the positives may be produced than the negatives. However, at mountain altitudes, this last effect is masked by the first two. All these effects are reversed in the west, and the net result is to favor the positives in that direction.

In the east, again due to the curvature, the negative mesons arise on the average from primaries incident at angles somewhat nearer the vertical than the angle of observation, while the reverse is true of the positives. Thus, the primaries which produce the negatives have, on the average, passed through less

absorbing material than those which produce the positives. Like the effects discussed in the preceding paragraph, this effect favors negatives in the east and positives in the west.

It has been noted above that intensities in different directions are different because of different values of  $M_c$ . This effect is such as to favor the west over the east for both positives and negatives, since  $M_c$  is always greater in the east than in the west for predominantly positive primaries. There is another, but very much smaller, effect of this kind, involving particles of opposite sign observed in the same direction. The negatives arise on the average from primaries incident in more westerly directions than the positives, that is, from directions where  $M_c$  is smaller. Hence, this effect tends to favor negative mesons in all directions, except very near the western horizon, where the negative trajectories intersect the earth.

Another quantity which affects the relative numbers of positive and negative mesons observed is what will be called the "positive excess at production." This is defined as the difference between the numbers of positives and negatives produced, divided by the average of the two numbers. It will be a function not only of the energy of meson produced, but also presumably will vary with the energy of the producing particle.

It can easily be seen that, because of the complexity of the phenomena involved, the observed "positive excess" in a given direction is only very indirectly related to that at production. Even at the vertical, where the discrepancy is least serious,

the observed excess depends to a considerable extent upon small terms in the expression for the  $\mu$ -meson intensities. The procedure, adopted by some investigators, of speaking in terms of a positive excess defined for a given zenith angle as

$$2(W_+ + E_+ - W_- - E_-)/(W_+ + E_+ + W_- + E_-),$$

where  $W_+$ , for example, represents intensity of positives in the west, is to be discouraged, as this quantity is of but doubtful significance.

Another quantity not susceptible of direct physical interpretation is the east-west asymmetry defined as  $2(W - E)/(W + E)$  for positives, negatives, or the natural mixture of both. In the last case (i.e., the natural mixture), it does approximate the effect due purely to the asymmetry of the primaries, although not exactly.

Since there are so many variables involved in the problem, naturally much more information can be gleaned from a study of the positives and negatives separately at various angles and at various energies. Groetzinger and McClure<sup>16</sup> measured the east-west asymmetries of positive and negative mesons for two different zenith angles at Mt. Evans, Colorado (geomagnetic latitude  $49^\circ$  N) and Chicago ( $51^\circ$  N). Both these locations are considered to be above the knee of the latitude curve, that is, they are sufficiently far north so that the cutoff rigidity  $M_c$  is low enough in all directions to admit essentially all primaries important in producing the observed secondary cosmic radiation. Thus

the asymmetries observed should be due only to the various effects of the curvature of the secondaries in the atmosphere after production. The experimental data are indeed consistent with such an interpretation, there being an asymmetry of positives toward the west, and a nearly equal asymmetry of negatives toward the east, of approximately the expected magnitude.

If the same observations are made at or near the equator, there is superposed upon the above asymmetries the effect of the large primary asymmetry at that latitude.

#### (b) Differential Range Spectrum of $\mu$ Mesons at Production

The number of mesons (positive and negative) of range between  $R'$  and  $R' + dR'$  produced in a given direction at a given level of the atmosphere per gram of material, per steradian of solid angle, per second will here be represented by  $G(R') \exp(-y/L)dR'$ , where  $G(R')$  is the differential  $\mu$ -meson production spectrum of Eq. (7),  $y$  is the quantity of matter in  $\text{g cm}^{-2}$  intervening between the point of production and the top of the atmosphere in the direction of production, and  $L$  is the absorption mean free path of the nucleonic component in  $\text{g cm}^{-2}$ .  $G$  depends, of course, upon the composition of the incident radiation, and hence upon latitude, longitude, zenith angle, and azimuth. Implicit in this representation is the assumption that the composition of the nucleonic component does not change significantly as it passes down through the atmosphere, but that it is merely attenuated exponentially.

To the extent that the spectrum of the primary radiat-

ion is really describable in terms of the single cutoff rigidity  $M_c$ , it is evident that  $a$  is a function of  $M_c$  only. This relationship is shown in Fig. 2 for the range of cutoff rigidities covered by Olbert's work. The ordinates of the points shown were taken from Olbert, <sup>3,4</sup> while the abscissas were computed by us, using Eq.(5), for the actual flight path followed in taking the data <sup>17</sup> upon which Olbert's figures are based. The values of the other two parameters have been taken, at least tentatively, directly from Olbert, viz.:

$$A = 7.31 \times 10^4 \text{ g}^{-2+n} \text{ cm}^{2-2n} \text{ sec}^{-1} \text{ sterad}^{-1}, n = 3.58.$$

Since we are here interested in the intensities of positive and negative mesons individually, it is necessary to consider two production spectra, which will be designated by  $G_\sigma(R'+a)$ , where  $\sigma$  is simply the sign of the meson,  $\pm 1$ . These are related to the positive excess at production  $\delta(R',a)$  and the total production spectrum  $G(R'+a)$  as follows:

$$G_\sigma(R'+a) \approx \frac{1}{2} \left[ 1 + \frac{1}{2} \sigma \delta(R',a) \right] G(R'+a). \quad (8)$$

### (c) Definitions

Before proceeding to a consideration of the intensities, it will be convenient here to define and explain certain of the quantities which will enter into the discussion:

H — depth of atmosphere at point of observation ( $\text{g cm}^{-2}$ ).

B — local horizontal terrestrial magnetic field (Gauss).

$\rho(Z)$  — density of atmosphere at vertical height  $Z$  above point of observation ( $\text{g cm}^{-3}$ ).

L --absorption mean free path of nucleonic component (taken to be  $121 \text{ g cm}^{-2}$ ).

$\mu$  --rest mass of the  $\mu$  meson ( $1.07 \times 10^8 \text{ ev/c}^2$ ).

$\tau$  --lifetime of the  $\mu$  meson ( $2.10 \times 10^{-6} \text{ sec}$ ).

q --charge of the meson ( $\pm e$ , the electronic charge).

R --residual range of meson at point of observation ( $\text{g cm}^{-2}$  air equivalent).

S --arc length upward along trajectory of meson from point of observation ( $\text{g cm}^{-2}$ ).

Z --vertical height in the upward direction from point of observation ( $\text{g cm}^{-2}$ ).

$\Theta$  --zenith angle of observation in east-west plane (considered positive if east of the vertical).

$\theta$  --zenith angle at point on trajectory, i.e., angle between tangent to curve and vertical at that point.

p --momentum of meson on arrival.

$p'$  --momentum of same meson at distance S along its trajectory.

$W_0(S,R)$  --probability of survival until observation of a  $\sigma$  meson produced at distance S on trajectory which would arrive at point of observation with range R.

#### (d) Computation of the Intensities at the Equator

In the discussion which follows, three assumptions have been made: (a)  $\pi$  mesons decay instantaneously, (b)  $\pi$  meson and  $\mu$ -meson production is collimated along the direction of flight of the original producing particle, and (c) multiple



scattering of  $\mu$  mesons in air is negligible.

For a detailed discussion of the range of validity of the above model, see reference 3. We shall return to these assumptions later.

In our case, we are interested specifically in the intensities of positive and negative  $\mu$  mesons at various zenith angles in the east-west plane. In view of the above model of  $\mu$ -meson production, we may write for these intensities

$$i_{\sigma}(R, \Theta) = \int_0^R G_{\sigma}(R + S + a) \exp\left(-\frac{H - Z}{L} \sec\Theta\right) w_{\sigma}(S, R) dS, \quad (9)$$

where the exponential expresses the absorption of the producing radiation, and the angle  $\Theta$  is not assumed to remain constant along the trajectory. The integration is carried from zero out to a point at which the survival probability has reduced the integrand essentially to zero.

It is possible to reduce Eq. (9) to the following form (see Appendix for details):

$$i_{\sigma}(R, \Theta) = C \cos^{n-1}\Theta J_1 \left[ 1 + \frac{1}{2} \sigma \bar{\delta}(R, a_t) \right] \\ \times \left[ 1 - \left(\frac{J_2}{J_1}\right) \left(\frac{\Delta}{H}\right) + \frac{1}{2} \left(1 + \frac{1}{n}\right) \left(\frac{J_2}{J_1}\right)^2 \left(\frac{\Delta}{H}\right)^2 \right] \\ \times \left[ 1 - \sigma \gamma \tan\Theta \left(\frac{J_4}{J_1}\right) - \sigma \gamma \left(\frac{J_6}{J_1}\right) \left(\frac{1}{H} \frac{da}{d\Theta}\right) \right], \quad (10)$$

where the following abbreviations have been made:

(a)  $C = \frac{1}{2} A (nH)^{-n}$ , (b)  $a_t = a(\Theta)$ , as distinguished from  $a=a(\theta)$ ,  
 (c)  $\gamma = e\tau B/\mu$ . The quantity  $\bar{\delta}(R, a_t)$  is the average positive excess at production of mesons arriving in direction  $\Theta$  with residual range  $R$ .

For computational purposes it was found convenient to express  $a_t$  as  $a_1 + \Delta$ , where  $a_1$  is an arbitrarily chosen central value of  $a$ , presumably intermediate between the values expected in the directions to be considered, and  $\Delta$  is a smaller quantity which is a function of  $\Theta$ .

The  $J$ 's which appear in Eq. (10) are all functions of  $R$  and  $\cos \Theta$ . They have been computed<sup>18</sup> for Chacaltaya (see Part IV, Sec. (b)), and are shown for  $\pm 45^\circ$  in Fig. 3 and for the vertical in Fig. 4. At  $45^\circ$  a value of  $621 \text{ g cm}^{-2}$  was used for  $a_1$ , while at the vertical it was  $640 \text{ g cm}^{-2}$ . The quantity  $J_4$  is absent at the vertical because there the term in which it occurs vanishes identically.

The constant  $C$  does not affect comparative intensity measurements taken at the same observatory. In addition, since the cosine is an even function of the angle, the multiplier

$$\cos^{n-1}(\Theta) J_1(R, \cos \Theta)$$

does not enter into east-west asymmetry measurements based on the differential intensities.

Because of the complexity of the theory, and because the survival probability and the curvature effects are expressible in terms of the same integrals (see Appendix), it has been impractical to try to keep separate all the effects which come into play

in determining the intensities. However, Eq. (10) does separate, for a given zenith angle in the east-west plane, the various causes leading to the observed asymmetries and the observed positive excesses.

The factor containing  $\delta(R, a_t)$  expresses the effect of the positive excess at production. The factor in which  $(J_2/J_1)$  occurs produces that part of the asymmetry directly traceable to the east-west asymmetry of the primary radiation. In the last factor, the term in  $(J_4/J_1)$  embodies the effect purely of the difference between the trajectories followed by positives and negatives, while the term in  $(J_6/J_1)$  is a hybrid, resulting from the variation in the primary radiation along the trajectory due to the change in slope.

#### IV. THE EXPERIMENT

##### (a) The Apparatus

A schematic end view of the apparatus used in the experiment to be described is shown in Fig. 5. The pieces marked I, II, III, and IV are long thin slabs of iron, each wound with several layers of heavy enameled wire. Sections I and II together form a complete magnetic circuit, being closed at the ends of the slabs by two pieces of the same material (not shown in the figure). Sections III and IV form a similar but separate magnetic circuit. In operation a magnetic field of 17000 gauss is maintained, having one sense in I and III, and the opposite sense in II and IV.

The counters, marked A, B, C, D, and X in the figure, have a 20 in. effective length, and are of  $\frac{9}{16}$  in. and  $\frac{15}{16}$  in. i.d., respectively. Those having the same literal designation have their outputs connected directly together.

The entire ensemble, magnets and counters, and another identical ensemble are mounted on axes parallel to those of the counters. The twin units can be swung separately to the vertical or to  $22\frac{1}{2}^{\circ}$ ,  $45^{\circ}$ , or  $67\frac{1}{2}^{\circ}$  from the vertical in either direction. The entire apparatus, in addition, can be rotated about a vertical axis and set at any desired azimuth.

In each case two threefold coincidences, (A,B,D) and (A,C,D), and two fourfold coincidences, (A,B,D,X) and (A,C,D,X), are counted. By taking directly the difference between readings of corresponding threefold and fourfold coincidences, one obtains the anticoincidence rates (A,B,D, - X) and (A,C,D, - X), i.e., for the former, those events in which there are simultaneous counts in A, B<sub>1</sub> or B<sub>2</sub>, and D, but no simultaneous count in any of the counters X. The two anticoincidence counting rates above will be referred to as channel I counting rate and channel II counting rate, respectively.

The apparatus tends to select either positive or negative particles, depending upon the direction of the current. Groetzinger and McClure,<sup>16</sup> with a closely similar apparatus, found the probability of traversal of a particle of the wrong sign to be negligible.

The sensitivity of a counter telescope to  $\mu$  mesons of

various ranges is describable in terms of an "acceptance function"  $r(R)$ . This function is so defined that, if the intensity of such particles  $i_0(R)$  is constant over the opening angle of the telescope, the number of particles per second having ranges between  $R$  and  $R + dR$  counted by the telescope is given by

$$dN_0(R) = r(R)i_0(R)dR. \quad (77)$$

Evidently, in our case there are two such functions,  $r_1(R)$  and  $r_2(R)$ , one for each channel. They are shown in Fig. 6.

In their computation, an approximate analytical expression for the range-momentum relation in iron and copper was used for those particles entering the apparatus in a plane perpendicular to the axes of the counters. For those particles entering at an angle to this plane, it was assumed that this angle remains constant during the motion, and that the projection of the trajectory in the plane is the same as the trajectory of a particle entering parallel to the plane and having the same average radius of curvature in the magnetic field. A large number of these trajectories was computed, and the necessary multiple integrations actually performed numerically.

The computation of Fig. 6 also took into account the effect of multiple scattering of the mesons in the material of the magnets. If one considers the paths of mesons known to pass through the two points A and B, separated by a distance  $x$ , the lateral distribution in space at the midpoint can be shown to be Gaussian, and it is possible to derive an expression for the mean square la-

teral displacement. <sup>79</sup> The spreading due to scattering was considered to be superposed upon the deflection due to the curvature in the magnetic field. The acceptance function is not very sensitive to the exact value of the mean square displacement, the effect being to "smear out" the acceptance function, making the peak lower and spreading it out laterally. An approximate value of mean square displacement was chosen for each value of range of the incident particle, assuming that the particles are incident at an "average" angle with the plane perpendicular to the magnetic field in the equipment. It can be shown that this angle is about  $13\frac{1}{2}^\circ$ .

Also included in Fig. 6 for comparison are the two other acceptance functions,  $r_1'(R)$  and  $r_2'(R)$ , which apply when there is no field in the iron. Note that these latter represent the sensitivity of the instrument to particles of either sign, not to those of one sign exclusively. They are due entirely to scattering. The zero-field counting rates are approximately one-sixth the sum of positive and negative counting rates in a given direction.

#### (b) Description of the Experiment

The apparatus has been operated at the Laboratorio de Física Cósmica on Mt. Chacaltaya, Bolivia since May, 1952. Certain data pertinent to this laboratory appear below:

$$\begin{aligned} \Lambda &= 16.4^\circ \text{ S}, & \gamma &= 4.8 \cdot 10^{-2}, \\ \Omega &= 68.0^\circ \text{ W}, & H &= 548 \text{ g cm}^{-2}, \\ \lambda &= 4.9^\circ \text{ S}, & \text{mean annual air pressure} &= 1103 \text{ mm Hg}, \end{aligned}$$



the vertical and at  $45^\circ$ . It has been assumed that all, or nearly all, the anticoincidence counts represent the passage of single  $\mu$  mesons through the apparatus. In channel I, the number of threefold coincidences is approximately twice the number of anticoincidence counts, while in channel II the threefold rate is some eight times the anticoincidence rate.

In order to compute the expected counting rates in our two channels, it is necessary to integrate Eq. (17) over all values of  $R$ . To do so, it is convenient to choose an average of  $\delta(R, \Theta)$  weighted, say, according to  $r(R) J_1(R, \cos \Theta)$ . This quantity will be denoted by  $\delta_1(\Theta)$  or  $\delta_2(\Theta)$ , depending upon the channel to which we refer. It has been tacitly assumed that since the cone of acceptance of the telescope is symmetrical about the direction of inclination of the magnet assembly,  $\Theta$ , the effect of the variation in intensity over the cone cancels out, at least in first order, and that therefore the effective intensity is that at zenith angle  $\Theta$ .

After the integrations over the acceptance function, mentioned in the preceding paragraph, the various terms occurring in the expression for  $i_r(R, \Theta)$  are found to have their counterparts in the expressions for the expected counting rates.<sup>18</sup> In our case, these counting rates will be represented by

$W_{\pm}, E_{\pm}, V_{\pm}, W_0, E_0,$  and  $V_0$  for each channel,  $W, E,$  and  $V$  indicating  $45^\circ$  west,  $45^\circ$  east, and vertical, respectively, and the  $\pm$  and  $0$  indicating polarity of the field in the iron or its absence.



The terms involving the derivative are very small and can be evaluated approximately using the curve of Fig. 2, extrapolated as shown to higher values of  $M_0$  in order to include directions east of the vertical. At Chacaltaya, the quantity  $(da / d\theta) / H$  has the following approximate values: 0.075 (45° west), 0.216 (vertical), and 0.613 (45° east).

Before proceeding to a comparison of the data with the theoretical expressions it must be noted that even if  $(\Delta / H)$ ,  $\delta_1$ , and  $\delta_2$  are known for each direction the observed counting rates will differ from those predicted by the theory in two principal ways:

First, there is a small number of spurious events which succeed in triggering the proper combination of counters. In events of this type, the incoming particle may pass through two of the three counters necessary for a coincidence, while the third counter is triggered by another particle ejected at an angle by the incoming particle, either in a nuclear disintegration or in a knock-on process. Alternatively, the first particle may pass through one counter and its product through two, etc. Hence the number of such counts should be practically independent of the direction, presence, or absence of the magnetic field in the iron. In addition, it should be roughly the same for both channels.

Second, a normalizing constant must be employed to correct for the error introduced in the computation of the acceptance functions by the many approximations it was necessary to make. Another fact which will affect the normalizing constant is that a

certain fraction of the particles passing through the proper three counters to cause a coincidence also produce knock-ons which trigger the anticoincidence counters, thus causing these events to be disregarded. The normalization is not necessarily the same for the two channels, nor for the zero-field case.

We shall assume that both these effects are present in some degree. It will also be assumed that  $\delta_1$  and  $\delta_2$  are unknown in all directions, that  $\Delta$  (and therefore  $a$ ) is unknown at  $45^\circ$  east and west, but that the value given by Fig. 2 for the vertical is correct.

From measured single and twofold coincidence rates, obtained by monitoring the equipment while in operation, it can be shown that corrections to the threefold and fourfold rates due to accidental coincidences and to counter dead time are entirely negligible.

There is a sufficient number of independent counting rates to evaluate the spurious counting rate, the normalization factors, and all the above unknowns. In fact, the problem is somewhat overdetermined, there being several counting rates not needed for the determination of the above quantities. This procedure yields the values of  $a$  shown on Fig. 2, plotted at  $M_c = 10.6$  and 23.3 Bv respectively, the corrected  $45^\circ$  west and east values at Chacaltaya. (The vertical value is 13.5 Bv, corresponding to  $a = 640 \text{ g cm}^{-2}$  on the curve.) The internal consistency of the data is excellent, as the superfluous counting rates are entirely compatible with the others, well within the experimental errors.

(d) Positive Excesses at Production

With the aid of Eq. (10), one can easily construct the observed positive excess in a given direction, as follows:

$$\epsilon(R, \Theta) = 2 \frac{i_+(R, \Theta) - i_-(R, \Theta)}{i_+(R, \Theta) + i_-(R, \Theta)}, \quad (12)$$

or, after simplification and neglecting certain very small terms in the denominator,

$$\begin{aligned} \bar{\delta}(R, \Theta) = \epsilon(R, \Theta) + 2\gamma \tan \Theta & \frac{J_4(R, \cos \Theta)}{J_7(R, \cos \Theta)} \\ & + 2\gamma \frac{J_6(R, \cos \Theta)}{J_7(R, \cos \Theta)} H^{-1} (da/d\Theta)_{\Theta}. \end{aligned} \quad (13)$$

Corresponding expressions for  $\delta_1(\Theta)$  and  $\delta_2(\Theta)$ , involving  $\epsilon_1(\Theta)$  and  $\epsilon_2(\Theta)$ , the observed excesses computed directly from the counting rates, and also involving the integrals of the  $J$ 's, can be derived.<sup>18</sup> It is worth noting that  $\delta_1$  and  $\delta_2$  can then be determined from the counting rates independently of the normalization, and are almost independent of the spurious rates, provided the latter are small. The  $\epsilon$ 's and  $\delta$ 's for the various directions are shown in Table I. The errors in the  $\delta$ 's shown are those corresponding to the statistical probable errors combined with an allowance for a possible 10% error in the computation of the numerical terms. However, the computations are seriously affected by the presence of small terms in the expression for the

intensities of positives and negatives in a given direction.

## V. MODIFICATIONS TO THE THEORY

Both  $a_W$  and  $a_E$  lie significantly below Olbert's curve (and its extrapolation, admittedly very uncertain). Physically, this means that all the intensities, both west and east, are rather higher than one would have expected in comparison with the vertical intensities. Of course, the points shown have been computed on the assumption that  $\Delta_V = 0$ , or in other words that  $a_V = 640 \text{ g cm}^{-2}$ . However, a change in the value assumed for  $a_V$  does not improve this situation appreciably. We have investigated this possibility and have found that, even if one assumes that the curve of Fig. 2 lies much higher or lower, the computed values of  $a_W$  and  $a_E$  will be raised or lowered by a very nearly equal amount, and will therefore not be brought much nearer the curve.

Since all our  $45^\circ$  counting rates have in effect been normalized to the vertical, we must seek some effect or effects which come into play at  $45^\circ$  in a different way from that at the vertical. The first such effect which comes to mind is the possible existence of negative primaries. The cutoff at the vertical as a function of geomagnetic latitude is the same for primaries of either sign, while east and west about the (corrected) vertical are interchanged for the two types of particles. Hence, asymmetries in the east-west plane at the equator would be reduced by the presence of any considerable number of negative primaries, below what would be expected assuming the primaries to be exclusively positive in

sign. Applied to our case, this means that  $a_w$  would lie above the curve derived from vertical data on the latitude effect, and  $a_E$  would lie below it. This is not adequate to explain the observed discrepancies.

In fact, disregarding the vertical data for the moment, one can compute, independently of the normalization, the asymmetries of positives and negatives on the assumption that  $a$  is really given by the curve and extrapolation of Fig. 2, i.e., that the western and eastern values are 609 and 746 g cm<sup>-2</sup> respectively. The results of this procedure are shown below,  $A_{\pm}$  being defined in the conventional way as  $2(W_{\pm} - E_{\pm}) / (W_{\pm} + E_{\pm})$ :

	Computed	Experimental
$A_+$ (channel I)	+0.447	+0.505 $\pm$ 0.018
$A_-$ (channel I)	+0.049	+0.110 $\pm$ 0.018
$A_+$ (channel II)	+0.534	+0.569 $\pm$ 0.037
$A_-$ (channel II)	+0.030	+0.069 $\pm$ 0.010

No error has been indicated for the calculated values, although this is presumably fairly large, due to the fact that the extrapolation of Fig. 2 is quite arbitrary. In view of this last fact, the above agreement must be considered good. If one hypothesizes that a certain fraction of the primaries is negatively charged, one may speculate as to the possible effect of this admixture on the calculated asymmetries. For example, in the event that the negative primaries may be considered completely symmetrical in

all their properties to the positive component of the radiation (that is, same rigidity spectrum, same multiplicity of  $\pi$ -meson production, negative excess at production of secondaries instead of positive excess, etc.), that portion of the  $\mu$ -meson intensity due to the positive fraction of the primary radiation can be computed as described above, while for that portion due to the negative fraction  $W_+$  and  $E_-$  are interchanged, etc.

Focussing attention on channel I, under the above conditions one computes by the method of the preceding paragraph the values 0.403 and  $-0.007$  for the two asymmetries if the fraction of negative primaries is 10%, and 0.359 and  $-0.063$  if it is 20%. In other words, as one assumes increasing numbers of negative primaries, the agreement with the experimental data becomes progressively poorer. The situation in channel II is not materially different. We take this as a strong indication for the absence of any considerable number of negatively charged particles in the primary cosmic radiation.

The second factor which can operate to make our normalization procedure give an erroneous result is the fact that we do not really observe the intensity at angle  $\Theta$ , but rather the average of the intensities taken from two cones of directions, one slightly to one side of  $\Theta$ , the other slightly to the opposite side. A Taylor's series expansion about  $\Theta$  yields the intensity at angle  $\Theta \pm \theta_1$ :

$$i(\Theta \pm \theta_1) = i(\Theta) \left[ 1 \pm \left( \frac{1}{i} \frac{di}{d\Theta} \right)_{\Theta} \theta_1 + \frac{1}{2} \left( \frac{1}{i} \frac{d^2i}{d\Theta^2} \right)_{\Theta} \theta_1^2 \pm \dots \right]. \quad (14)$$

If we interpret  $\theta_1$  as the magnitude of the angle which the central direction of the cone of observation makes on each side with the direction  $\Theta$ , the observed intensity is the average of the two intensities of Eq. (14), or

$$\bar{i} = i(\Theta) \left[ 1 + \frac{1}{2} \left( \frac{1}{i} \frac{d^2 i}{d\Theta^2} \right) \theta_1^2 + \dots \right]. \quad (15)$$

The term involving the first derivative cancels out in the averaging, and the fractional magnitude of the effect on the intensity at  $\Theta$  is therefore

$$\frac{1}{2} \left( \frac{1}{i} \frac{d^2 i}{d\Theta^2} \right) \theta_1^2.$$

The next term (that in the fourth power of  $\theta_1$ ) and all higher even power terms are negligible.

Biehl, Neher, and Roesch<sup>27</sup> investigated the zenith angle dependence of the local cosmic radiation in the east-west plane at the geomagnetic equator over Peru. From their curves for atmospheric depth  $310 \text{ g cm}^{-2}$  and 20.8 cm of lead absorber, one can make a crude estimate of the effect in our case. In channel I of our apparatus it is of the order of 0.4% to 2.0%, while in the other channel the effect is about three times as large. In neither case is the effect large enough to account for the unexpectedly large counting rates at  $45^\circ$ .

The third possible explanation is that the assumptions involved in the highly simplified model of  $\mu$ -meson production here employed must be re-examined. It is possible that the meson-producing component of the cosmic radiation does not vary strictly exponentially with atmospheric depth, especially in the uppermost

part of the atmosphere. If this is the case, it is difficult to estimate the effect on our computations. However, at these altitudes, very considerable proportions of the observed mesons arise at all levels above that of observation, and it is hard to imagine that such an effect could account for more than one or two percent in the normalization.

The effect of the scattering of the mesons will be similar to that discussed in connection with  $\theta_1$ , but it is even smaller, the root-mean-square scattering angle being of the order of only  $3^\circ$

A significantly larger effect results from the lack of collimation in the production of mesons. Observations in photographic emulsions at high altitudes <sup>22</sup> indicate that most  $\pi$  mesons having minimum ionization produced in nuclear events are collimated in a cone of about  $15^\circ$  half-angle about the direction of the primary particle.

The maximum angle of emission in the laboratory system of a  $\mu$  meson whose parent  $\pi$  meson has momentum  $p_\pi$  can be calculated straightforwardly. The parent of our "typical"  $\mu$  meson has  $p_\pi / m_\pi c = 20$  (very approximate), corresponding to a maximum angle of emission of about  $1^\circ$ . This is negligible in comparison with the spreading which occurs in the primary collision.

Thus  $\mu$  mesons produced at angle  $\theta$  at a certain point along the trajectory leading to detection in the apparatus arise from primaries not in the direction  $\theta$ , but rather in a cone of directions surrounding that of the trajectory at that point. Let us, for simplicity, consider only the variation in the east-west plane,



at least for the inclined directions. For a pair of angles  $\theta \pm \theta_2$  distributed symmetrically about  $\theta$ , the intensities of the primary radiation at a certain point are proportional to

$$\exp \left[ - \left( \frac{H - Z}{L} \right) \sec (\theta \pm \theta_2) \right],$$

where, however, we have neglected the small variation of  $a$  between  $\theta - \theta_2$  and  $\theta + \theta_2$ . This function can be expanded in a series about  $\theta$ , and the resulting two intensities averaged. As before, the term in the first derivative vanishes, and we can write for the over-all average of the intensities over the cone of incidence of the primaries

$$\bar{I} = I(\theta) \left\{ 1 + \frac{1}{2} \left( \frac{H - Z}{L} \right) \sec \theta \right. \\ \left. \times \left[ \left( \frac{H - Z}{L} \right) \sec \theta (\sec^2 \theta - 1) - (2 \sec^2 \theta - 1) \theta_2^2 \right] \right\}, \quad (16)$$

where now  $\theta_2$  must be interpreted as the root-mean-square angle of spread in the production of  $\pi$  mesons, projected into the east-west plane. At the vertical, the situation is slightly different because of the cylindrical symmetry about that direction, and we must use the root-mean-square angle in space.

Examination of Eq. (16) indicates that one needs some sort of average value of both  $(H - Z)/L$  and  $(H - Z)^2/L^2$ . The appropriate ones are the averages weighted according to the relative numbers of mesons produced at various heights, or, to a high order of approximation, according to the function  $\Psi(Z, R, \cos \Theta)$  de-

defined in the Appendix. If one computes the numerical values of these two averages for a residual range of  $600 \text{ g cm}^{-2}$  (central value for channel I) and substitutes the trigonometrical factors for the vertical and for  $45^\circ$ , one obtains the fractional effects (on the intensities one would have in the case of perfect collimation) as follows:

$$- 0.85\theta_2^2 \text{ (vertical); } + 0.14\theta_2^2 \text{ (}45^\circ\text{)}.$$

The coefficient at the vertical is always negative, but its magnitude is to some extent a function of R because of the dependence of the "distribution-in-production height" of observed mesons on R.

At  $45^\circ$ , however, the situation is more complex. Here, at high altitudes the curve of primary intensity vs zenith angle is concave downward, while at lower altitudes a point of inflection intervenes, and the curve is concave upward. Hence, for low residual ranges, where the distribution function favors the lower altitudes, the coefficient is positive, while for higher ranges (greater than about  $700 \text{ g cm}^{-2}$ ) the coefficient is negative.

It is interesting to note that Olbert actually determined the production spectrum of  $\mu$ -mesons produced in the vertical direction, rather than the production spectrum corresponding to primaries incident at the vertical. It is the latter quantity which is of more fundamental interest. Olbert's spectrum, which can be derived from it through application of the correction given above, is usable to a good order of approximation provided one considers vertical data only. However, when one tries to apply his

production spectrum to data at zenith angles other than zero there will be serious discrepancies. Since the vertical effect is negative, our "real" production spectrum will differ from Olbert's "effective production spectrum at the vertical" in that the normalizing constant  $A$  will be somewhat greater.

As before noted, the correction does depend on  $R$ , and therefore it is not strictly correct to apply a simple numerical correction to Olbert's constant  $A$  in order to find its "true" value. Evidently, there will be some effect on the constants  $n$  and  $a$  as well. We suggest that it would be highly advisable, when sufficient data exist, to repeat Olbert's computation of the  $\mu$ -meson spectrum, taking this last effect into account in detail.

We shall be content for the present to modify Olbert's normalization in such a way that his spectrum coincides with the "true" one for range  $R = 600 \text{ g cm}^{-2}$ . It is worthy of note at this point that, at least to a first order of approximation, the much smaller effects due to  $\theta_1$  and to scattering of the mesons in air can be lumped together with  $\theta_2$ . Another effect, which is important at the vertical but not at  $45^\circ$ , is that due to the distribution of the solid angle to the north and south of the east-west plane. The root-mean-square angle between the incoming trajectory and the east-west plane is about  $16 \frac{1}{2}^\circ$ , and its effect, too, can be approximately lumped with  $\theta_2$ .

Let it be assumed, for the moment, that  $a_w$  actually lies on the Olbert curve. It is then possible to compute, within certain accuracy, using the channel II zero-field data at the ver-

tical and at  $45^\circ$  west, the spurious rates at the vertical and at  $45^\circ$ . One can then derive from the channel I data with field, vertical and  $45^\circ$ , both the root-mean-square angle of production of  $\pi$  mesons needed to bring the  $45^\circ$  and vertical data into accord and the corresponding value of  $a_E$ . The angle needed is  $14^\circ \pm 2^\circ$ , a value certainly not inconsistent with the observations of Brown et al.,<sup>22</sup> and the value of  $a_E$  obtained is  $785 \pm 5 \text{ g cm}^{-2}$ , a point lying not too far from the tentative extrapolation of the curve used until now.

We consider this result, taken conjointly with the foregoing considerations, to be sufficient justification for assuming that  $a_w$  actually does lie on the curve. One would, of course, not expect perfect agreement with the extrapolated portion of the curve, as it is highly arbitrary. Olbert's curve has been extended in Fig. 2 to include the point at  $45^\circ$  east, obtained as described above.

We are now in a position to attempt the crude modification of Olbert's production spectrum mentioned above. Using the angle  $14^\circ$  characteristic of the  $\pi$ -meson production, which brought about the best agreement of our results with Olbert's work, one finds for the " $\theta_2$  effect" at the vertical at sea level - 5.4%. (This figure does not include any possible effect due to the finite opening angle of the equipment used in obtaining the data upon which Olbert's computations are based.) We may now conclude that, in order to obtain the "true" production spectrum, at least in the region of range  $R = 600 \text{ g cm}^{-2}$ , we must modify Olbert's

constant A as follows:

$$A' = A / (1 - 0.054). \quad (17)$$

We find thus that A must be increased from  $7.37$  to  $7.73 \times 10^4$ . Now, according to Olbert,<sup>2,3</sup> the average depth of production of mesons arriving at sea level with range  $600 \text{ g cm}^{-2}$  is about  $213 \text{ g cm}^{-2}$ , and since sea level corresponds to an atmospheric depth of  $1033 \text{ g cm}^{-2}$ , the average range of such particles at production is some  $820 \text{ g cm}^{-2}$  greater than that at observation, or about  $1400 \text{ g cm}^{-2}$ . Hence we conclude that the "true" production spectrum  $G(R')$ , at least in the vicinity of  $R' = 1400 \text{ g cm}^{-2}$ , is given approximately by

$$G(R') = 7.73 \times 10^4 [R' + a(Mc)]^{-3.58} \quad (\text{g}^{-2} \text{ cm}^2 \text{ sec}^{-1} \text{ sterad}^{-1}), \quad (18)$$

where  $a(Mc)$  is given by Fig. 2 Note that Eq. (18) is now considered to hold anywhere on the earth's surface and in any direction of incidence.

It is now possible to compute a new set of theoretical counting rates for our apparatus, based on the corrected production spectrum and the values of  $a_w$  and  $a_E$  taken from the correct  $a(Mc)$  curve of Fig. 2, and corrected for the  $\theta_2$  effect. The latter is slightly different for channel II from the values given above, due to the fact that the "typical" meson has a different range. These theoretical counting rates are shown, for both channels, in table IV.<sup>23</sup> Also shown are the experimental rates, corrected for

spurious counts and the equipment normalization. It was necessary to recompute the normalization factors, which are shown, together with the original spurious rates, in Table II.<sup>23</sup> Table IV indicates which of the data have been used to compute the various parameters of the theory. The values of the positive excesses at production shown in Table I are not affected by the above corrections.

It is clear from Table IV that the theory is adequate to explain all the observed counting rates. Work is soon to be undertaken on an analysis of data taken at zenith angles of  $22\frac{1}{2}^{\circ}$  and  $67\frac{1}{2}^{\circ}$ . It is hoped that the results of this analysis will provide confirmation of the theory developed in this paper.

For the purpose of comparison with other experiments the conventionally measured east-west asymmetries  $A$  for positives, negatives, sum of positives and negatives, and zero-field are tabulated in Table III. It is noteworthy that, where the statistical accuracy admits of direct comparison, the asymmetry of the sum of positives and negatives agrees very well with the asymmetry measured with zero field, thus confirming our interpretation that the particles detected in the latter case consist of a "natural mixture" of positives and negatives scattered in the iron of the magnets. Both these figures can be compared, at least qualitatively, with the results of Biehl, Neher, and Roesch.<sup>21</sup> They found, over Peru, a total asymmetry which increased with increasing absorber thickness (i.e., with increasing energy of the observed particles), and which decreased with increasing atmospheric depth. Their result at  $45^{\circ}$ , with 20.8 cm of lead absorber at  $310 \text{ g cm}^{-2}$  atmospheric

Table I. Positive excesses observed ( $\epsilon$ ) and at production ( $\delta$ ).

Direction	$\epsilon_1$	$\delta_1$	$\epsilon_2$	$\delta_2$
45° west	$+0.300 \pm 0.017$	$+0.172 \pm 0.021$	$+0.301 \pm 0.067$	$+0.121 \pm 0.069$
45° east	$-0.104 \pm 0.021$	$+0.103 \pm 0.028$	$-0.212 \pm 0.089$	$+0.070 \pm 0.092$
vertical	$+0.073 \pm 0.008$	$+0.091 \pm 0.008$	$+0.075 \pm 0.028$	$+0.100 \pm 0.028$

Table II. Normalization factors and spurious counting rates

Spurious counting rate - either channel

Vertical	$1.01 \pm 0.35$ hr <sup>-1</sup>
45°	$0.50 \pm 0.10$ "

Normalization factor - vertical or 45°

channel I (field on)	$0.830 \pm 0.011$
channel I (field off)	$0.790 \pm 0.014$
channel II (field on)	$0.979 \pm 0.029$
channel II (field off)	$0.977 \pm 0.158$

Table III. East-west asymmetry A conventionally measured.

Type of measurement	Channel I	Channel II
positive particles	$+ 0.505 \pm 0.018$	$+ 0.569 \pm 0.037$
negative particles	$+ 0.110 \pm 0.018$	$+ 0.069 \pm 0.040$
positive + negatives	$+ 0.321 \pm 0.017$	$+ 0.330 \pm 0.069$
zero field	$+ 0.312 \pm 0.044$	$+ 0.244 \pm 0.405$

Table IV. Comparison of experimental and theoretical counting rates  
(All in  $\text{hr}^{-1}$ ).

Channel	Direction	Sign	Theoretical counting rate (corrected)	Experimental counting rate (corrected and normalized)	Notes
I	45° west	+	16.31	$16.31 \pm 0.27$	1,2
I	45° east	+	9.73	$9.73 \pm 0.19$	1,2
I	45° west	-	12.05	$12.05 \pm 0.21$	1,2
I	45° east	-	10.78	$10.78 \pm 0.20$	1,2
I	45° west	o	4.42	$4.30 \pm 0.14$	
I	45° east	o	3.12	$3.14 \pm 0.12$	
I	vertical	+	26.24	$26.24 \pm 0.49$	1,2
I	vertical	-	24.40	$24.40 \pm 0.46$	1,2
I	vertical	o	7.86	$8.05 \pm 0.35$	
II	45° west	+	3.27	$3.18 \pm 0.16$	2
II	45° east	+	1.77	$1.77 \pm 0.13$	2
II	45° west	-	2.42	$2.35 \pm 0.14$	2
II	45° east	-	2.19	$2.19 \pm 0.14$	2
II	45° west	o	0.53	$0.45 \pm 0.13$	3
II	45° east	o	0.36	$0.35 \pm 0.12$	
II	vertical	+	5.17	$5.42 \pm 0.39$	2
II	vertical	-	4.80	$5.03 \pm 0.39$	2
II	vertical	o	0.91	$1.10 \pm 0.40$	3

Note 1. Data used in the determination of  $a_0$  and also the root-mean-square angle of  $\pi^-$  meson production, needed in the correction of the theory. Apparent perfect agreement is, therefore, to be expected here.

Note 2. Comparative values of positive and negative counting rates but, not absolute values, used for determination of positive excesses.

Note 3. Data used for approximate determination of spurious counting rates.



depth, most nearly approximates the conditions of our data, with a total asymmetry of  $0.304 \pm 0.015$ . Our data were taken at rather greater atmospheric depth, but corresponded to particles of rather higher energy, and in channel I the sum of positives and negatives gave  $0.321 \pm 0.017$ .

We are grateful to Professor Bruno Rossi, under whose guidance this work was performed.

#### APPENDIX

The purpose of this appendix is to outline the derivation of Eq. (10) of the text.

The change in direction of a  $\mu$  meson due to curvature in the earth's magnetic field as we proceed upward a distance  $ds$  along its trajectory is

$$d\theta = (\sigma eB/p) (ds/\rho). \quad (19)$$

This expression yields, upon integration,

$$\theta - \theta_0 = \sigma \gamma a \quad (20)$$

where the following abbreviations have been made:

$$e\sigma B/\mu = \gamma \quad (21)$$

$$\frac{1}{\sigma c} \int_0^S \frac{\mu c}{p(R+S)} ds = \frac{ds}{\rho(Z)} = a \quad (22)$$

The probability of survival of the meson from the point of production to the point of observation can also be expressed in terms of the latter quantity, as follows:

$$\mathcal{W}_0(S,R) = \exp(-\alpha). \quad (23)$$

It is convenient in what follows to refer all computations to a "zero-order trajectory," i.e., we expand all variables, their functions, and integrals about the values they would have if the mesons came in along a straight line trajectory in the direction in which they are observed. The subscript  $t$  will be used to indicate such quantities.

In order to evaluate  $\alpha$ , it is convenient also to have an analytical expression for the range-momentum relation of  $\mu - m_e$  mesons in air, and we shall here employ that found by Olbert<sup>2</sup>:

$$\mu c/p_t = \psi(R_t) = \eta(b+R_t)^{-1} - \kappa \quad (24)$$

The values of the constants in Eq. (24) are as follows:  $\eta = 53.5 \text{ g cm}^{-2}$ ,  $b = 56 \text{ g cm}^{-2}$ ,  $\kappa = 2.07 \times 10^{-3}$ .

Now  $dS$  is given by  $dZ \sec\theta$ , and also approximately, for angles  $\theta$  near  $\theta_0$

$$\sec\theta = \sec\theta_0(1 + \tan\theta_0 \sigma \gamma \alpha). \quad (25)$$

If one expands  $\psi(R_t)$  about the "zero-order trajectory," one obtains

$$\psi(R') = \psi(R'_t) + (S' - S'_t) \psi'(R'_t), \quad (26)$$

where  $R'_t = R + S'_t = R + Z' \sec \Theta$ .

By means of Eqs. (20), (24), (25), and (26) it is possible to obtain,<sup>18</sup> after considerable manipulation and substitution, the following expression:

$$a = a_0 + \frac{1}{2} \tan \Theta \sigma \gamma a_0^2 - \tan \Theta \sigma \gamma \times \int_0^{a_0(Z)} \left[ \frac{\int_0^{Z'} a_0(Z'') dZ''}{Z' + \ell} \right] da_0 - \lambda_0 \sec \Theta, \quad (27)$$

where

$$\ell = (R+b) \cos \Theta, \quad (28)$$

$$a_0 = (\eta/\tau c) \int_0^Z (Z'+\ell)^{-1} [dz'/\rho(Z')], \quad (29)$$

$$\lambda_0 = (K/\tau c) \int_0^Z [dz'/\rho(Z')]. \quad (30)$$

It is to be noted that the quantity  $\gamma$  giving the magnitude of the local magnetic field is quite small (never more than about  $6 \times 10^{-2}$ ) compared with unity and that also, due to the small magnitude of  $K$ , the integral  $\lambda_0$  is quite small compared with  $a_0$ . Thus  $\lambda_0$  can be considered to be of the order of  $\gamma a_0$ . The function  $a_0$  itself is of the order of unity. Therefore, in the derivation of Eq. (27), terms of the order of  $\gamma^2 a_0$  and  $\gamma \lambda_0$ , and all smaller terms, have been neglected.

The integral  $\alpha_0$  is a function of vertical height  $Z$ , and depends parametrically upon the quantity  $\ell$  defined in Eq. (28) above. In other words, for a given location on the earth's surface, a family of curves of  $\alpha_0$  vs  $Z$  can be constructed with  $\ell$  as a parameter.<sup>18</sup>

These curves then serve, at least in the east-west plane for computations at any zenith angle. Note that  $\ell$  is symmetrical about the vertical.

The other integral  $\lambda_0$  is simply a function of  $Z$ , and a single curve is adequate to express the relationship at any particular location on the earth.<sup>18</sup>

Both integrals depend on the density distribution in the atmosphere above the point of observation. Hence, since

$$\frac{1}{\rho(Z')} = \left( \frac{R}{Mg} \right) \frac{T(Z')}{H - Z'}, \quad (31)$$

where  $T(Z')$  is the absolute temperature,  $R$  is the universal gas constant,  $M$  is the average molecular weight of air, and  $g$  is the acceleration of gravity, they likewise can be considered functions of the temperature distribution in the atmosphere, and computed as follows:

$$\alpha_0 = \left( \gamma / \tau c \right) \left( R/Mg \right) \times \int_0^Z (Z'+\ell)^{-1} (H - Z')^{-1} T(Z') dz', \quad (32)$$

$$\lambda_0 = (K/\tau c) (R/Mg) \int_0^Z (H-Z')^{-1} T(Z') dZ'. \quad (33)$$

It is more convenient to work with the temperature than directly with the density, as the former is known directly from meteorological data. The temperature distribution is a function of geographic latitude, and it is therefore not possible to compute universal curves for  $\alpha_0$  and  $\lambda_0$ . The distribution is, however, quite constant throughout the equatorial regions. It is shown for this region in Fig. 7, as taken from Olbert.<sup>3</sup>

Equation (9) can be rewritten as

$$i_\sigma(R, \theta) = \frac{1}{2} \int_0^H \left[ 1 + \frac{1}{2} \sigma \delta(R', a) \right] \times G(R'+a) \exp \left( - \frac{H-Z}{L} \sec\theta - \alpha \right) \sec\theta dZ. \quad (34)$$

The positive excess at production  $\delta$  is a number rather less than unity, and presumably does not vary very rapidly with  $R'$  and  $a$ . Therefore, any difference in  $\delta$  along the curved path from that computed along the zero-order trajectory must be negligible, and we have  $\delta(R', a) = \delta(R'_t, a_t)$ . Eqs. (25) and (27) can be substituted into Eq. (34), and the small terms in  $\gamma$  removed from the exponential through use of the expansion  $e^x \approx 1+x$ .

It is advisable, for computational purposes, to expand the function  $G(R'+a)$  about the value it takes on when  $a$  is equal to some arbitrarily chosen central value  $a_1$ , in terms of the deviation of the true value of  $a$  from this central value.

To this end, we write

$$a_t = a_1 + \Delta(\Theta). \quad (35)$$

The choice of  $a_1$  in a practical case is dictated by considerations of convenience. If  $a$  is known in the vertical direction, that figure might be a good choice for  $a_1$ . At any rate, some value intermediate between those expected for  $a$  in a given application should be used. The value of  $a$  along the trajectory differs from  $a_1$  also to a very small extent due to the deviation of  $\Theta$  from  $\Theta$  along the trajectory. It is then possible to expand  $G(R+a)$  as follows:

$$\begin{aligned} G(R+a) &= G(R_t' + a_1) \\ &\times \left\{ 1 - \xi_1 \left[ \frac{\Delta \cos \Theta}{H} + \frac{(S' - S_t') \cos \Theta}{H} \right. \right. \\ &\left. \left. + \frac{1}{H} \frac{da}{d\Theta} (\Theta - \Theta) \cos \Theta \right] + \frac{1}{2} \left( 1 + \frac{1}{n} \right) \right. \\ &\left. \times \xi_2 \left[ \left( \frac{\Delta \cos \Theta}{H} \right)^2 + \frac{2(S' - S_t') \Delta \cos^2 \Theta}{H^2} \right] \right\}, \quad (36) \end{aligned}$$

where  $\xi_1$  is the following function:

$$\xi_1 = nH \left[ Z + (R+a_1) \cos \Theta \right]^{-1}. \quad (37)$$

After substitution of Eq. (36) into Eq. (34), and some further manipulation and simplification, one obtains an expression of the following form for the intensities:

$$i_{\sigma}(R, \Theta) = \frac{1}{2} A (nH)^{-n} \cos^{n-1} \Theta \int_0^H \left[ 1 + \frac{1}{2} \sigma \delta(R'_t, a_t) \right] \times \Psi(Z, R, \cos \Theta) [1 + \text{other terms}] dZ, \quad (38)$$

where

$$\Psi(Z, R, \cos \Theta) = \int_1^n \exp \left[ - \left( \frac{H-Z}{L} - \lambda_0 \right) \sec \Theta - a_0 \right]. \quad (39)$$

Now  $\frac{1}{2} \delta$  is quite small compared to unity, and hence if we define a weighted average of  $\delta$  as

$$\bar{\delta}(R, a_t) = \frac{\int_0^H \Psi(Z, R, \cos \Theta) \delta(R'_t, a_t) dZ}{\int_0^H \Psi(Z, R, \cos \Theta) dZ}, \quad (40)$$

we may write to an excellent order of approximation

$$i_{\sigma}(R, \Theta) = \frac{1}{2} A (nH)^{-n} \cos^{n-1} \Theta \left[ 1 + \frac{1}{2} \sigma \bar{\delta}(R, a_t) \right] \times \int_0^H \Psi(Z, R, \cos \Theta) [1 + \text{other terms}] dZ. \quad (41)$$

The integral in Eq. (41) can be evaluated numerically term by term, and the result, after further manipulation,<sup>18</sup> is Eq. (10) of the text.

1. M. Sands, Phys. Rev. 77, 180 (1950)
2. S. Olbert, Phys. Rev. 92, 454 (1953)
3. S. Olbert, ~~Technical~~ Report No 61 Laboratory for Nuclear Science, Massachusetts Institute of Technology, 1954 (unpublished).
4. S. Olbert, Phys. Rev. 96, 1400 (1954).
5. C. Störmer, Z. Astrophys. 1, 237 (1930)
6. E. J. Schremp, Phys. Rev. 54, 158 (1939).
7. G. Lemaitre and M.S. Vallarta, Phys. Rev. 49, 719 (1936).
8. G. Lemaitre and M.S. Vallarta, Phys. Rev. 50, 493 (1936).
9. G. Lemaitre and M.S. Vallarta, Phys. Rev. 43, 87 (1933).
10. W. F. G. Swann, Phys. Rev. 44, 224 (1933).
11. For curves of proton energies corresponding to  $M_1$  and  $M_2$  in various directions, see M.S. Vallarta, Phys. Rev. 74, 1837 (1948).
12. J. Bartels and S. Chapman, Geomagnetism (Oxford University Press, 1940), p. 651.
13. B. Rossi, Atti. accad. nazl. Lincei 15, 62 (1932).
14. T. H. Johnson, Phys. Rev. 59, 11 (1941).
15. I. S. Bowen, Phys. Rev. 45, 349 (1943).
16. G. Groetzinger and G.W. McClure, Phys. Rev. 77, 777 (1950).
17. M. Conversi, Phys. Rev. 79, 750 (1950).
18. F. B. Harris, thesis, Massachusetts Institute of Technology, January, 1955 (unpublished).
19. See e.g., B. Rossi, High-Energy Particles (Prentice-Hall, New York, 1952), p.72.
20. U. S. Coast & Geodetic Survey, Magnetic observations in the American Republics (U. S. Dept. of Commerce, Washington, D.C. 1946), Serial 677.
21. Biehl, Neher, and Roesch, Phys. Rev. 76, 914 (1949).
22. Brown, Camerini, Fowler, Heitler, King, and Powell, Phil. Mag. 40, 862 (1949).
23. Certain of the quantities in Tables IV and II differ slightly from their counterparts in reference (13), because the method for evaluating some of the parameters of the theory has since been somewhat improved from a statistical standpoint.



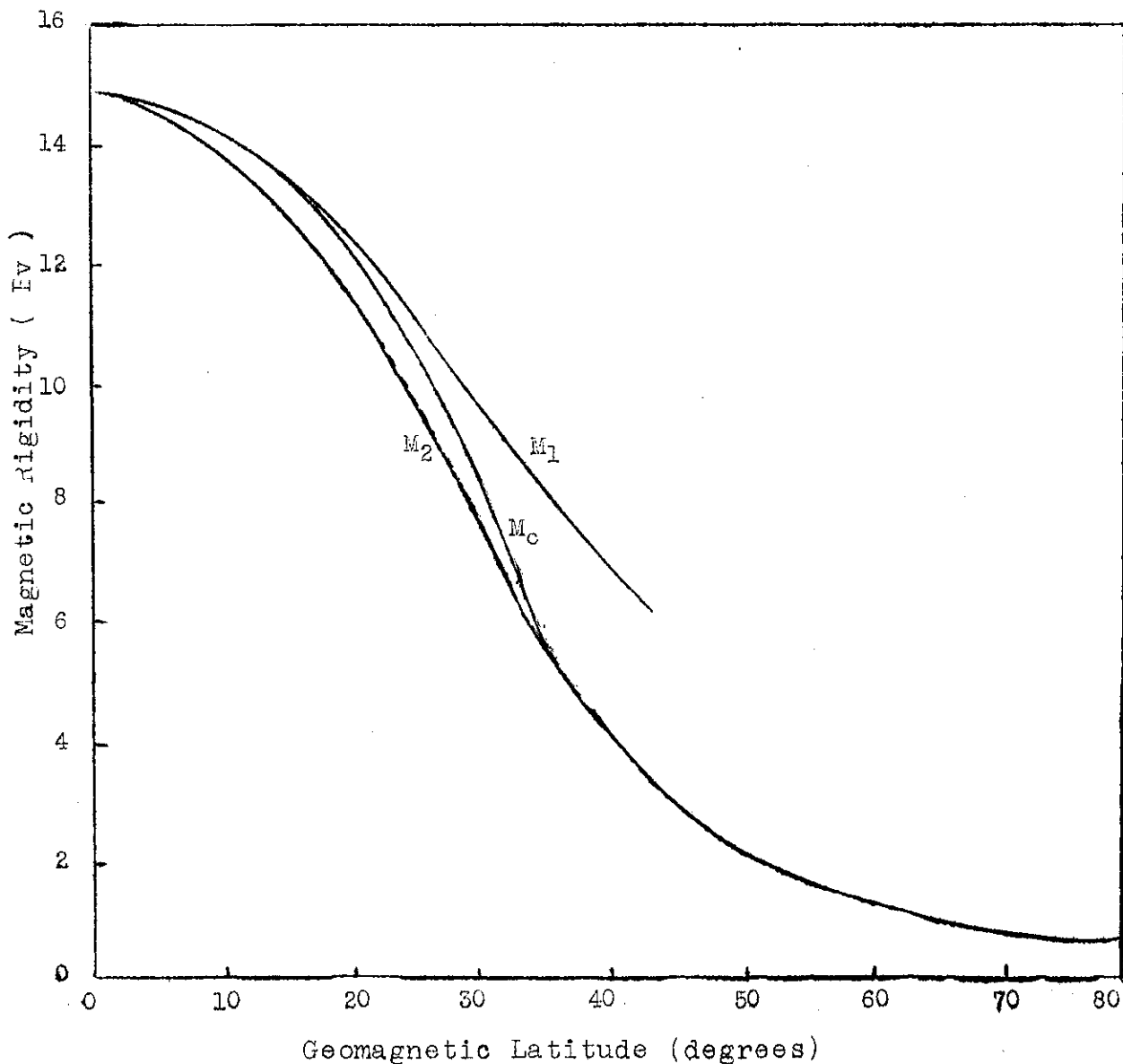


Fig. 1. The three critical magnetic rigidities,  $M_1$ ,  $M_2$  and  $M_c$ , in the vertical direction, uncorrected for eccentricity of the earth's dipole, as functions of geomagnetic latitude. At a given latitude, particles of all rigidities greater than  $M_1$  arrive vertically, while no particles of rigidities less than  $M_2$  can arrive.  $M_c$  is a tentative equivalent "cutoff" rigidity producing, as nearly as possible, the same secondary effects as the true spectrum of primaries.

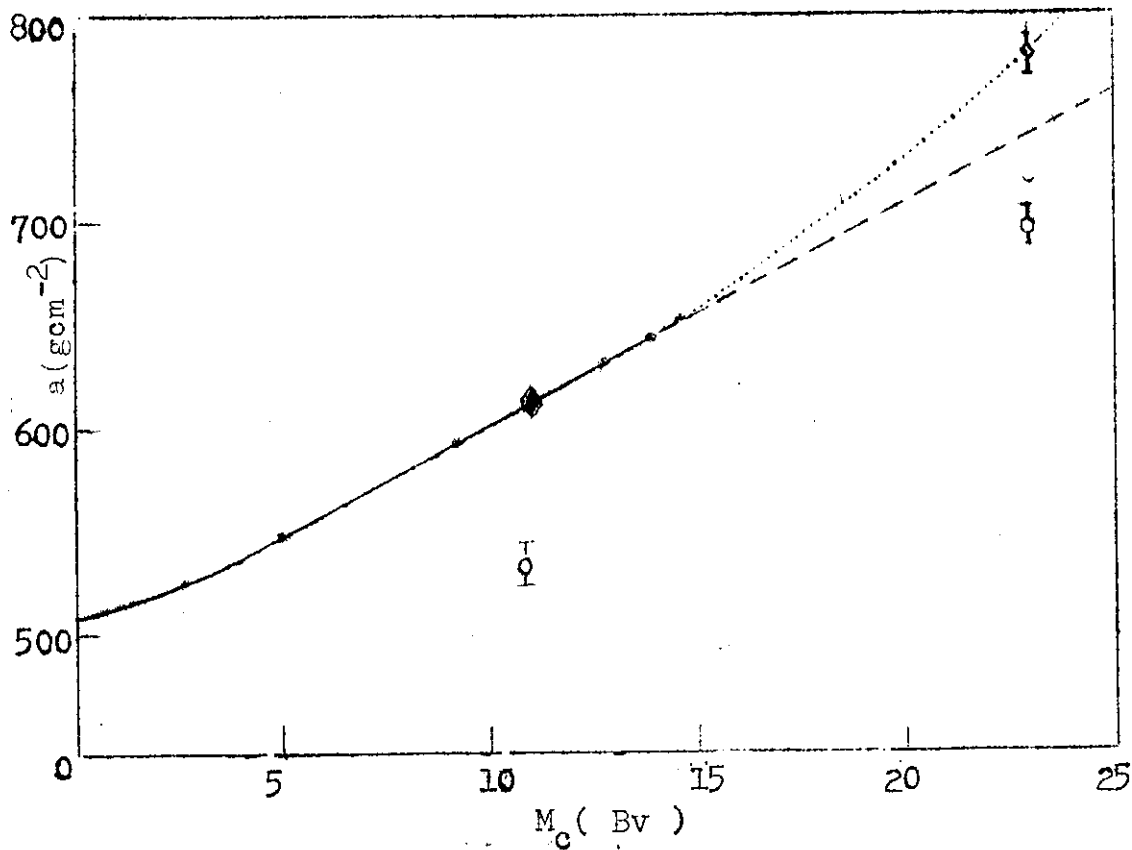


Fig. 2. The parameter  $a$  occurring in the expression for the production spectrum  $G(R')$ , as a function of cutoff rigidity  $M_c$ . The solid curve was derived from Olbert's results in the vertical direction. His points are shown by solid circles. The dashed curve represents the tentative extrapolation of this curve used in the early stages of the analysis.

The values of  $a_W$  and  $a_E$  obtained with the uncorrected theory are shown by hollow circles. The solid diamond indicates the value of  $a_W$  under the assumption that the latter lies on the curve, while the hollow diamond indicates the value derived for  $a_E$  on the basis of the same assumption. The dotted curve then represents the corresponding extension of Olbert's curve.

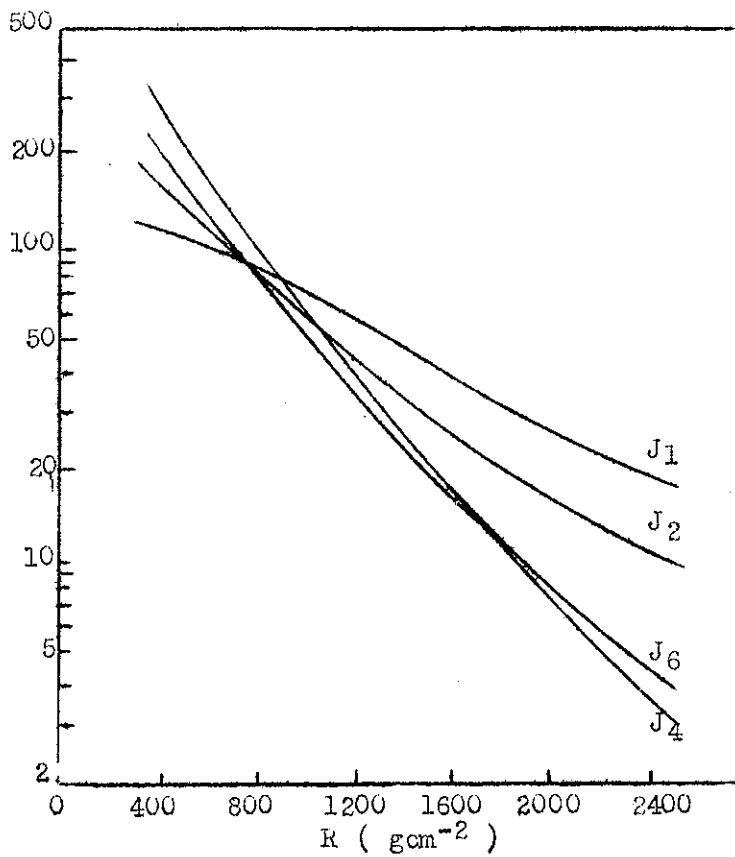


Fig. 3. The functions  $J_i(k, \cos \theta)$ , in terms of which the intensities  $i_\sigma(R, \theta)$  are expressible, computed for  $\theta = \pm 45^\circ$ .

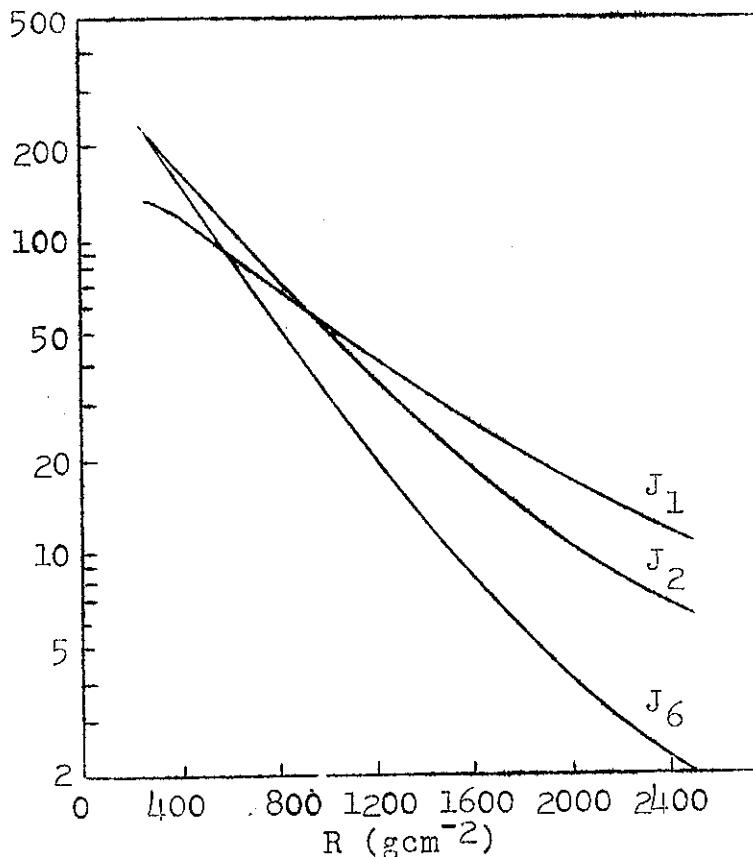


Fig. 4. The functions  $J_i(R, \cos \theta)$ , in terms of which the intensities  $i_g(k, \theta)$  are expressible, computed for  $\theta = 0^\circ$

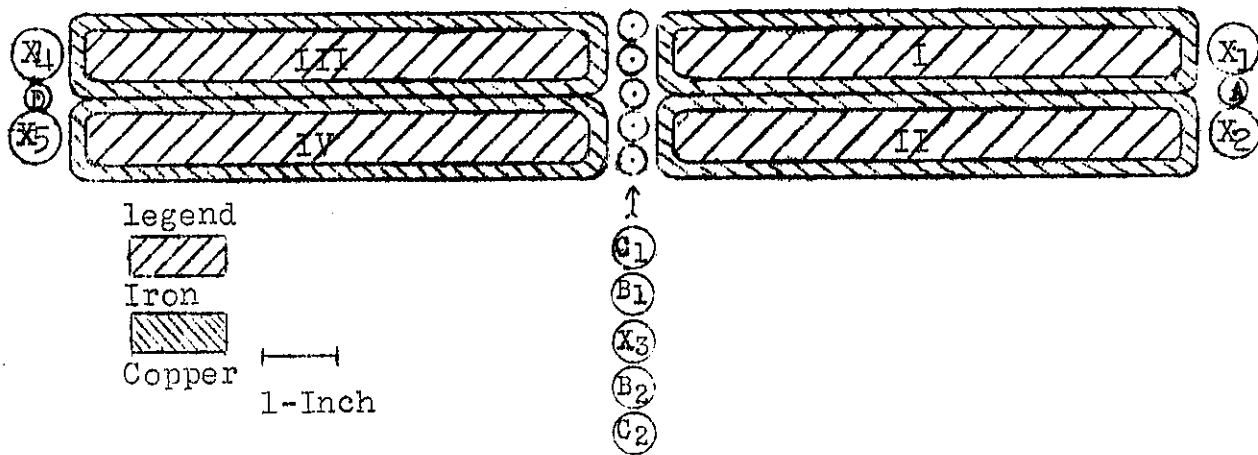


Fig. 5. End view of one of the two identical magnet arrangements. The smaller circles represent 5/8 in. Geiger tubes, the larger ones 1-in. tubes. For clarity, the iron end pieces completing the two magnetic circuits ( viz., I-II and III-IV ) have been omitted from the figure.

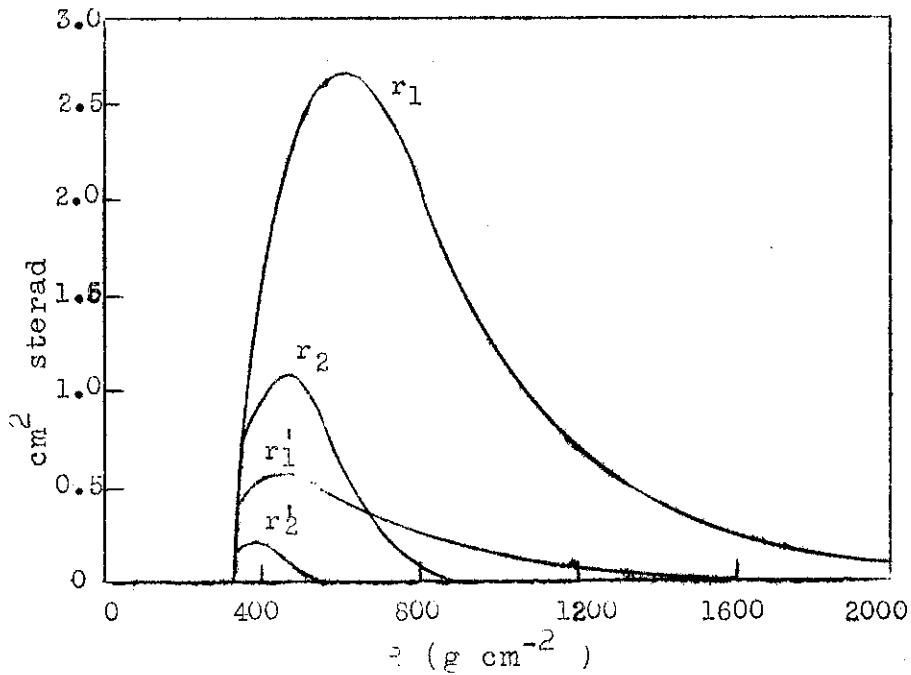


Fig. 6. Acceptance functions of one magnet assembly.  $r_1$  and  $r_2$  apply to particles of one sign only accepted by channels I and II, respectively, with field in the magnets on.  $r_1'$  and  $r_2'$  apply to particles of any sign accepted by channels I and II, respectively, with field in the magnets off.

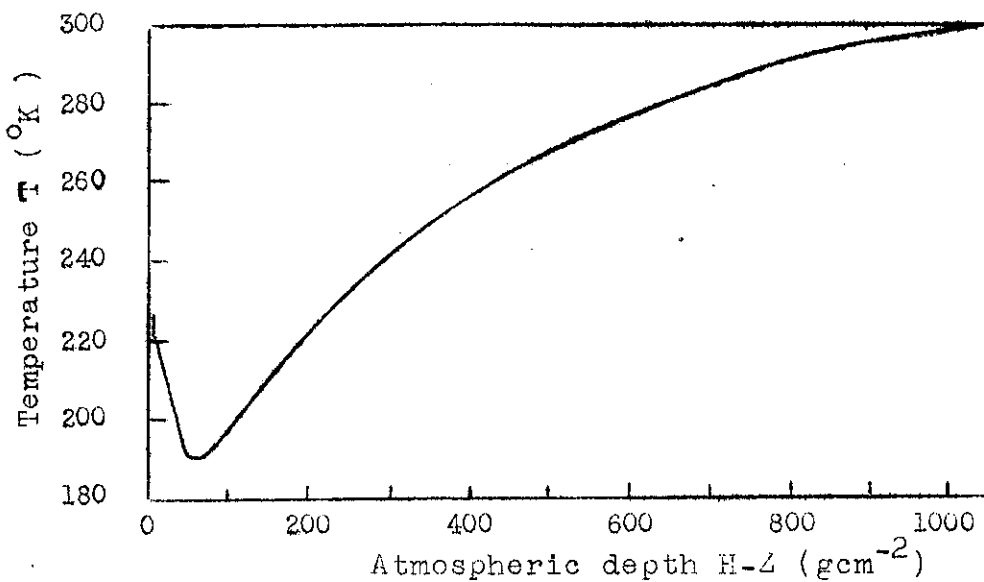


Fig. 7. Annual mean temperature of the atmosphere in the equatorial regions as a function of atmospheric depth H-Z .